Analyst

Accepted Manuscript

ROYAL SOCIETY OF CHEMISTRY

www.rsc.org/analyst

Cite this: DOI: 10.1039/c0xx00000x

www.rsc.org/xxxxxx

ARTICLE TYPE

Oligopeptide-heavy metal interaction monitoring by hybrid gold nanoparticles based assay

Jane Politi [a,b], Jolanda Spadavecchia*[b,c], Mario Iodice [a], Luca de Stefano [a]

Received (in XXX, XXX) Xth XXXXXXXXX 20XX, Accepted Xth XXXXXXXXX 20XX

DOI: 10.1039/b000000x

Phytochelatins are small peptides that can be found in several organisms, which uses these oligopeptides to handle heavy metal elements. Here, we report a method of monitoring interactions between lead (II) ions in aqueous solution and Phytochelatin 6 oligopeptides bioconjugated onto pegylated gold nanorods (PEG-AuNr). This study is the first step towards a high sensitive label free optical biosensor to quantify heavy metals pollution in water.

1. Introduction.

Nanostructured materials have become increasingly popular due to their unique properties as well as their promising breakthrough in development of novel biosensors for medical diagnostics, and environmental monitoring [1-3]. In recent years, gold nanoparticles have been widely applied in biosensor devices due to their unique size-dependent optical properties [4-6]. Therefore, more attention should be paid to find efficient synthesis methods to match the enlarging demand of gold nanoparticles (AuNPs). Several different solution synthesis methods have been employed to prepare gold nanoparticles, including biomolecule reduction of $HAuCl_4$ [7], seed mediated synthesis at room temperature [8] and polymer-assisted synthesis [9]. Recently, the utility of nanomaterials for any application is strongly dependent upon their physicochemical characteristics and their interactions with surfaces modifiers. Let's recall the importance of stabilizers, used in the synthesis of nanoparticles, not only to protect particles against aggregation but also to control their functional properties. Biver et al. [10] synthesized Au nanoparticles are using thioalkylatedoligoethylene glycols and functionalized with various fluorescent Acridine Orange derivatives [11]. Exchange of organic molecules on Au nanoparticles with PEG can indeed be performed to prepare biocompatible PEG-stabilized Au nanoparticles [12]. Wang et al. synthesized a Polyethylene glycol (PEG)-modified gold nanoparticle complex by one-step reaction by synchrotron x-ray irradiation method [13]. A low concentration of unmodified PEG macromolecules is very important to control particle size and stabilize gold nanoparticles demonstrate high stability under realistic biomedical conditions [14]. Other approaches were applied to stabilize gold nanoparticles using sulfur-containing polymers, with a possible limitation of their suitability for specific biomedical application. Self-assembling of biomolecular probes with free thiol groups on gold nanoparticles surface is allowed by well-known specific interactions, such as the Au-SH bond, thus avoiding complex chemical procedures for covalent conjugation [15, 16]. Some studies [17-19] showed that gold nanoparticles can interact with specifically sequenced peptides that can self-assemble on their surface. The polypeptides could induce or prevent aggregation of nanoparticles causing consequently the change of absorbance and, moreover, allow to interact with other metal ions i.e. Cd^{2+}, Ni^{2+}, Co^{2+}, Zn^{2+} etc. Lead is a widely used heavy metal and has a large number of industrial applications, such as battery manufacture, paint, gasoline, alloys, radiation shielding, piping and so on. Lead content in paints and gasoline represents a severe risk of environment pollution and, consequently, for human health. Lead is toxic by ingestion and inhalation, and can seriously affect the gut and the central nervous system, and it can also cause anemia [20, 21]. Furthermore, overexposure to lead can also cause birth defects, mental retardation, behavioral disorders, and death in fetuses and young children [22, 23]. Beside the social impact, detection and quantization of lead contamination is not an easy task since water is a complex matrix and any method proposed should be not only sensitive but also highly selective: lead content should be determined in presence of lot of interference substances, without any pre-treatment of the collected sample. This is the reason why bioprobes having high specific affinity with this metal must be used. Some oligopeptides, named Phytochelatins (PCs), with structural relation to Glutathione (γ-Glu-Cys-Gly) have been widely studied because of their ability to chelate heavy metal ions in plants and fungi for detoxification mechanisms [24, 25]. PCs are formed by dipeptide γ-Glu-Cys repeated from 2 to 11 times followed by a final Gly, so as their general structure is $(\gamma\text{-Glu-Cys})_n\text{Gly}$. We report here synthesis to prepare polymer-modified gold nanoparticles and gold nanorods using dycarboxylic PEG (DPEG) as stabilizer. We have thus implemented and evaluated a simple and reproducible method for labeling biomolecules with PEG gold nanostructures without utilizing organic solvents and surfactants. A new kind of pegylated gold nanorods based assay to quantify lead-Phytochelatin 6 (PC6) interactions in aqueous solution by using the oligopeptides as bioprobes was developed. Ultraviolet-visible (UV-Vis) spectroscopy and Fourier transform surface plasmon

resonance (FT-SPR) has been used for monitoring the formation of metal-biological complexes at different concentration lead.

2.Experimental

2.1. Materials.

Tetrachloroauric acid (HAuCl4), sodium borohydride (NaBH4) and ethanol (C2H5OH), polyethyl-ene glycol 600 Diacid (DPEG; Mw= 600 Da), cetyl-trimethyl ammonium bromide (CTAB), β-Mercaptoethylamine (cysteamine), N-hydroxysuccinimide (NHS), 1-(3-dimethylaminopropyl)-N'-ethylcarbodiimide hydrochloride (EDC), PBS (phosphate buffer solution, pH 7.2), lead (II) methanesulfonatesolution were purchased from Sigma Aldrich. Phytochelatin 6 (PC6) was purchased from Anaspec IGT group.All chemicals were used without any further purification.Gold substrates for FT-SPR meas-urements were deposited at IMM-CNR in Lecce (Italy).

2.2. Synthesis of Pegylated Au nanorods (PEG-AuNRs). The synthesis of pegylated gold nanorods (PEG-AuNRs) was performed following the well established seed-mediated procedure, in the presence of CTAB and DPEG in growth solution. Seed solution (S): seeds particles were prepared following the method described elsewhere [26, 27]. Briefly, 5 mL of CTAB (0.20 $molL^{-1}$) were added to 5 mL of an aqueous solution containing $HAuCl_4$ (2.5 x 10^{-4} $molL^{-1}$) under stirring conditions at room temperature. 0.6 mL of ice–cooled $NaBH_4$ (0.01 $molL^{-1}$) was then added. Growth solution (G): Growth solution was prepared by adding 5 mL of CTAB (0.02 $molL^{-1}$) to a solution of 0,75mL of DPEG and stirring for 10 min at room temperature. After 10 min 0.25 mL AgNO3 (4 x 10^{-3} $molL^{-1}$) , 5 mL of $HAuCl_4$ (1 x 10^{-3} $molL^{-1}$) were transferred to the mixture for 5 min. After this time, 70µl of ascorbic acid (8 x 10^{-3}M) was added. The synthesis of PEG hybrid gold nanorods (AuNr) was achieved as follows: 12µl of gold seed solution (S), was transferred to the growth solution (G), at room temperature conditions.

2.2.1Synthesis of Pegylated Au nanoparticles (PEG-AuNPs). Li et al. [28] have reported a facile method to synthesize AuNPs from concentrated chloroauric acid by adding sodium hydroxide in the presence of citrate as stabilizer. We modified this protocol by adding dicarboxylic PEG as surfactant, in the mixture reaction . Briefly, 25 mL of Chloroauric acid ($HAuCl_4$) aqueous solution (2.5 x 10^{-4}M) was added to 0.25mL of DicarboxylicPEG and mixed by magnetic stirring for 10 min at room temperature. To this solution, 20 mL of aqueous 0.01M $NaBH_4$ was added at once. The formation of the PEG-AuNPs was observed as an instantaneous color change of the solution from pale yellow to bright red after addition of the reducing agent. The as-prepared PEG-AuNPs solution was centrifugated at 15.000 rpm for 26 min for three times and then the supernatant was discarded and the residue was redispersed in an equivalent amount of buffer solution (PBS pH: 7). This was repeated twice principally to remove excess of dicarboxylic PEG. Stock solutions were stored at 27-29°C and characterized using UV-Vis spectroscopy and transmission electron microscopy (TEM).

2.2.2.Bioconjugation of PEG-AuNr and PEG-AuNPs with PC6. The gold nanorod surface was modified with PC6 peptides according to the following procedure (see scheme 2). 0.5 mL of the PEG-AuNrand PEG-AuNPs in a buffered solution (PBS, pH: 7.2) were added into separate tubes containing 0.5 mL of PC6 (0.7µM). Next, the AuNr-AuNPs/PC6 suspension was centrifuged twice at 6000 rpm for 20 min to remove excess of protein and then the pellets were redispersed in 1mL MilliQ water. The resultant colloidal solution was sonicated for 5 min and then stirred for 1 h at room temperature. Scheme 1 depicts the gold nanospheres and nanorods bioconjugation.

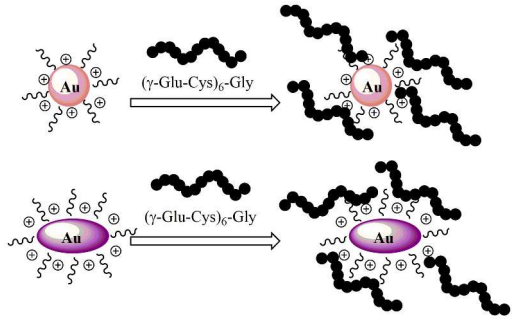

Scheme 1. Ionic interaction mechanism of PC6 protein grafting onto gold nanospheres (above) and gold nanorods (below).

2.2.3.PC6 immobilization on gold substrates. For PM-IRRAS analyses, glass substrates (11 x 11 mm^2), successively coated with a 5 nm thick layer of chromium and a 200 nm thick layer of gold, were purchased from Arrandee (Werther, Germany). The gold-coated substrates were annealed in a butane flame to ensure a good crystallinity of the topmost layers and rinsed in a bath of absolute ethanol for 15 min before use. Chemistry procedures based on SAMs of β-mercaptoethylamine (cysteamine) in absolute ethanol have been described previously [29]. Briefly, the freshly cleaned gold substrate was immersed in an unstirred 10 mM ethanol cysteamine solution of at room temperature, in the dark, for 6 h. The gold substrate was then washed with ethanol and ultrapure water (Milli-Q, Millipore, France) to remove the excess of thiols. The cysteamine-modified gold substrates were immersed in a EDC/NHS (80mg/20mg)-PC6 and PC6-AuNr solutions for 1h and then rinsed with phosphate buffer solution and MilliQ water three times for 5 minutes.

2.2.4.Lead (II) detection. Interaction between PC6-AuNr and lead (II) solutions was followed using UV-Vis spectra (50µL lead solution added to 1mL PC6-AuNr solution to obtain final lead concentration of 100, 50 and 25 ppb) and FT-SPR shifts of PC6-modified gold substrates.

2.3.Instrumentation

2.3.1.UV/Vis measurements. Absorption spectra were re-corded using a Jasco V-570 UV/VIS/NIR Spectrophotometer from Jasco Int. Co. Ltd., Tokyo, Japan in the 200-800 nm range.

2.3.2.TEM imaging. Transmission electron microscopy measurements were recorded on a JEOL JEM 1011 microscope operating at an accelerating voltage of 100 KV. The TEM graphs were taken after separating the surfactant from the metal particles by centrifugation. Typically 1mL of the sample was centrifuged for 20 min at a speed of 14000 rpm/min. The upper part of the colourless solution was removed and the solid portion was re-dispersed in 1 ml of water. 2 µL of this redispersed particle

suspension was placed on a carbon coated copper grid and dried at room temperature.

2.3.3.PM-IRRAS. PM-IRRAS spectra were recorded on a commercial Thermo (Les Ulis- France) Nexus spectrometer. The external beam was focused on the sample with a mirror, at an optimal incident angle of 80°. A ZnSe grid polarizer and a ZnSe photoelastic modulator, modulating the incident beam between p- and s-polarizations (HINDS Instruments, PEM 90, modulation frequency = 37 kHz), were placed prior to the sample. The light reflected at the sample was then focused onto a nitrogen-cooled MCT detector. The presented spectra result from the sum of 128 scans recorded at a 8 cm^{-1} resolution.

2.3.4.FT-SPR. FT-SPR measurements were performed with an SPR 100 module from Thermo equipped with a flow cell mounted on a goniometer. It was inserted in a Thermo-scientific Nexus FT-IR spectrometer using a near-IR tungsten halogen light source. The incidence angle was adjusted to have the minimal reflectivity located at 9500 cm^{-1}, at the beginning of each experiment, so as to be in the best sensitivity region of the InGaAs detector. Interactions between nanostructured surfaces and lead solution was carried out in the test chamber (10 µL/min; T = 27° C).

3.Results and discussion.

3.1.Synthesis of PEG-AuNps and PEG-AuNr. It is well established that PEG-functionalized AuNPs have an increased stability in aqueous and biological media with respect to simple gold nanoparticles [26, 30]. In order to improve the biointerfacial properties of AuNPs, we coated them with a bifunctional PEG linker carrying two carboxylic groups. The synthesis of PEG-capped gold nanoparticles (DPEG-AuNPs) was achieved by reducing-tetrachloroauric acid ($HAuCl_4$) with sodium borohydride ($NaBH_4$) in the presence of PEG-diacid as a capping agent. The main difference with other synthesis procedures of DPEG-AuNPs is that PEG-diacid is used in the same way as the citrate for the stabilization of the particles through electrostatic interactions between the carboxylic acid groups and the gold surface [28]. Particle formation and growth were tuned by the amphiphilic character of the PEG-diacid polymer and include three steps: (1) reduction of $HAuCl_4$ facilitated by dicarboxylic acid-terminated PEG to form gold clusters; (2) adsorption of PEG diacid molecules on the surface of the gold clusters and reduction of metal ions in that vicinity; and (3) growth of gold particles and colloidal stabilization by PEG polymers. The TEM picture of PEG-AuNPs highlights well and monodisperse Au nanospheres with a mean size of 7.2 nm with a standard deviation of 2 nm Figure 1(left). The growth of gold nanostructures, synthesized by seed-mediated procedure, is known to be strongly dependent on the seed nanocrystal structure, the latter being influenced by the nature of surfactants [31]. In the present study, the influence of PEG diacid molecules on the growth nanostructures was investigated. Based on the literature, the protocol conducted in the absence of PEG diacid at any step, is expected to lead to the formation of gold nanorods [26,32].

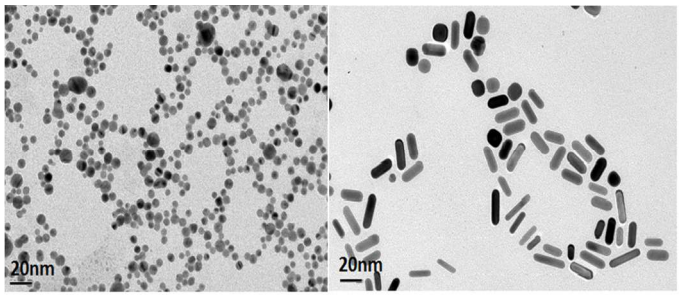

Figure 1. Transmission Electronic Microscopy images of AuNPs (left) and AuNr (right).

Figure 1 (right) reports TEM images which confirm the morphology and the remarkable dispersion of the nanorods, with a typical diameter of ca 5 nm and a length of ca 20 nm. Figure 2 displays the LSPR bands of AuNr: the UV-Vis spectrum shows a strong resonance band at around 780 nm corresponding to the longitudinal plasmon oscillation, and a weaker one at ca 530 nm corresponding to the transverse plasmon oscillation band confirming the presence of elongated gold nanorods, well isolated from each other, in agreement with previous published findings [33]. In a remarkable review, Pèrez-Juste et al., have clarified the role of CTAB concentration and temperature upon the nanoparticle aspect ratio, based on a large set of experimental results [33]. In particular, these authors proposed that the binding of Au ions, and thus the growth of Au nanorods in aqueous surfactant solution, are controlled by the electric field around the CTAB micelles [34]. In the present study, CTAB present in the seed solution is supposed to be in the micellized form, as the concentration used is significantly higher than the critical micelle concentration, reported to be equal to 0.92 mM [35]. When PEG diacid are added in the growth solution , leading to the formation of a presumable CTAB-PEGdiacid complexes, the same reduction process involving ascorbic acid may occur. The further reduction of Au can then proceed via an electron transfer at the surface of electron-rich, CTAB-PEGdiacid capped, seed particles. The rate of hybrid NPs formation, depends in this case on the reaction of $AuCl_2^-$-CTAB-PEGdiacid complex with CTAB-PEGdiacid capped seed particles that confer more stability in aqueous medium.

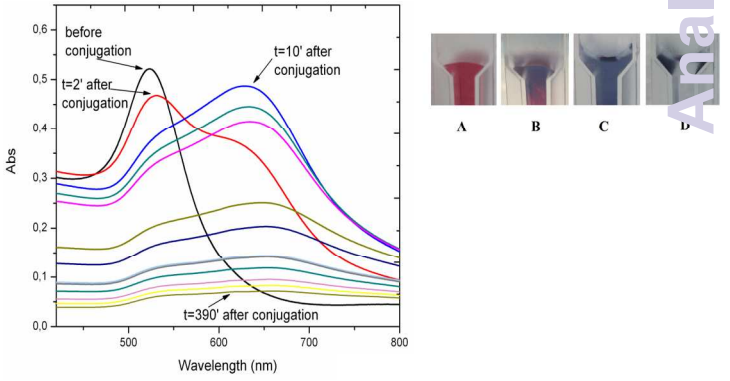

Figure 2. On the left: Uv-Vis spectra of PC6-modified AuNPs as function of time; on the right: images of AuNPs color changing during bioconjugation.

3.2.PC6 Adsorption onto pegylated gold nanostructures (PEG-AuNPs, PEG AuNr). Interaction of PC6 biomolecules and gold nanoparticles (PEG-AuNPs) or nanorods (PEG-AuNr) was monitored by observing the Localized Surface Plasmon (LSP) band in the UV–Vis spectrum. Figure 2 displays the LSP bands of AuNPs before and during interaction with PC6 molecules at equal concentrations of AuNPs in aqueous solution (10^{-4} M). It is well visible that AuNPs before adsorption show one peak at 530nm and their water solution has a typical red-rose color (Figure 2-A), while after 2 minutes of mixing with PC6 peptides, a strong color change can be clearly observed (Figure 2-B and C), which corresponds to the appearance of a second LSP peak around 650nm. UV-Vis spectra were recorded up to 390 minutes after PC6 molecules interaction but just after 120 minutes the hybrid biological-metal complex becomes instable, since the solution turns transparent (Figure 2-D), due to agglomeration and sedimentation of nanoparticles. Figure 3 shows the variation of absorption peaks of PEG-AuNr before and after binding with PC6.

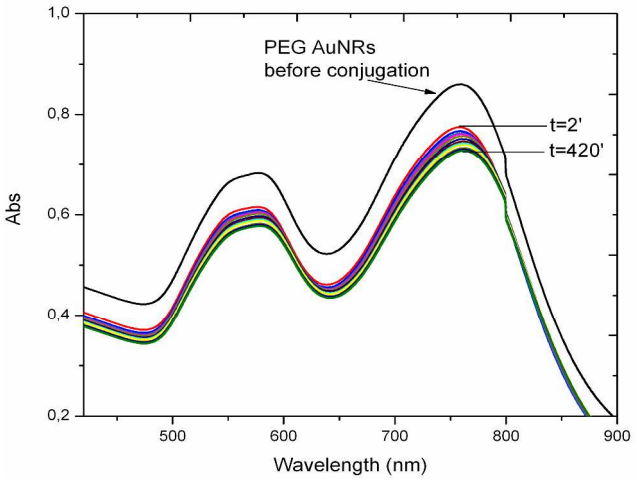

Figure 3. UV-Vis spectra of AuNr before and after bio-conjugation wih PC6 protein.

These measurements were carried out at room temperature during 18h. The violet color of PEG-AuNr solution resulting after interaction of PC6 did not change any more. A decrease of the plasmon absorption can be attributed to the change of localized refractive index near the AuNr surface indicating that PC6 were attached to the AuNr surface. From UV-Vis recorded spectra, it is clear that AuNr bind PC6 molecules and the resulting complexes are stable since there is not any degradation of the absorption peak. We remark that the stability of PEG-AuNr is due to the presence of two different capping agents, such as DPEG and CTAB respectively. After their synthesis, gold nanorods carry positive and negative charges on their surfaces due to strongly adsorbed CTA^+-PEG-COO^- ions, preferentially along the side surfaces. PC6 may adsorb to the PEG-AuNr sides via electrostatic attractions. As a matter of fact, with positively charged CTAB, PC6 likely interacts via its negative charges, thus exposing neutral, or positively charged, groups towards the external sides. Conversely, on PC6 interacting with the end of nanorods, charges are evenly distributed thus favoring classical Van der Waals inter-phytochelatin interations. We do not exclude the interaction of COO^- groups of DPEG with positive charges of PC6 onto gold nanorods: the mechanism for peptide assembly is probably triggered by electrostatic interactions between the depronated DPEG and the positively charged CTAB surfactant bilayer on the surface of gold nanorods, as a consequence of the improvement of AuNr stability. A better stability and evaluation of PEG-AuNr bioconjugation was confirmed by PM-IRRAS, which is particularly useful in case of very thin layer of modified materials. Planar gold surfaces were functionalized by a cysteamine self-assembled monolayer, which could strongly bound, under EDC/NHS chemistry activation, PC6 in one sample, and PC6-AuNr in another sample, for comparison purposes (see scheme 2).

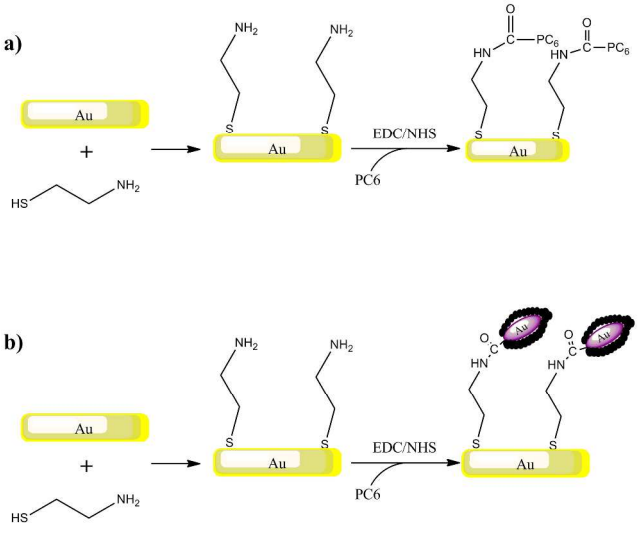

Scheme 2. Schematic representation of the biosensor elaboration strategy: Au surface modification with cysteamine self-assembled monolayer and PC6 (a) or PC6-modified gold nanorods (b).

Figure 3 shows a set of PM-IRRAS data taken after protein immobilization on the gold surface (Figure 3 black line) and after PC6 conjugated PEG-AuNr immobilization on the gold surface (Figure 4 redline). Spectrum PEG pattern is confirmed by vibrations band of the (C-O-C) at 1020 cm^{-1},the C=O stretching mode of the carboxylic group expected at 1725 cm^{-1} is evidenced. The peak at 1420 cm^{-1}, were attributed to the asymmetric and symmetric C-H scissoring vibrations of CH_3-N^+ moieties and to the CH_2 scissoring mode, respectively. In PM-IRRAS spectra, the peak at 1750cm^{-1} is assigned to ester bonds, as a consequence of EDC/NHS activation, the peak at1660cm^{-1} owns to the amide II bonds and the one at 1530cm^{-1}, to the amide I bonds: in both cases all the peaks are comparable, except for the peak at 1020cm^{-1}characteristic of C-O-C chain of PEG that confirms a good interaction between PC6 and PEG-AuNr.

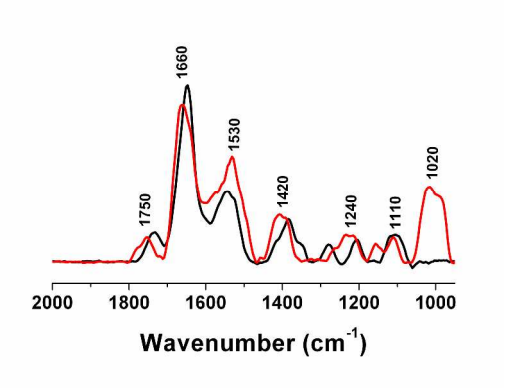

Figure 4. PM-IRRAS spectra of PC6-modified gold substrates (black line) and PC6-AuNRs-modified gold substrates (red line).

3.3.Interaction of PC6-AuNRs with lead (II) ions. FT-SPR measurements were used in monitoring interaction between PC6-AuNRs and lead (II) ions. Figure 5-A shows the real-time monitoring of all Pb (II) solutions with different concentrations tested. At instant t=64 min, a solution of lead ions with 100ppb concentration was injected into the test flow chamber, producing a shift of the FT-SPR peak absorption to 8650 cm^{-1}; then an aqueous solution was flown in order to wash the SPR surface, and the FT-SPR signal restored at its starting value at 9320 cm^{-1}. At t=93 min, a solution of lead ions at 50ppb concentration was injected, producing a shift of FT-SPR up to 9050 cm^{-1}; then aqueous solution was flown again to rinse the surface. At t=115 min, a solution of lead ions at 25ppb concentration was injected yielding a FT-SPR wavenumber value of about 9100 cm^{-1}; finally aqueous solution was flown to rinse the surface. It is of particular interest that after rinsing the signal restores its initial value since this means that interaction between nanocomplexes and metal ions is reversible. These wavenumber shifts indicate that lead (II) ions in solution significantly bind to phytochelatin modified AuNr even if the hybrid probes are conjugated to the analysis surface of FT-SPR. Figure 5-B reports how the absolute position of the plasmon absorbance peak changes as a function of different concentration of lead ions solution, while Figure 5-C shows data obtained from relative shifts of plasmon peak during exposition to Pb (II) ions solutions. These data could be fitted using OriginLab Software ™ by the following equation (Boltzmann model):

$$y=A2+((A1-A2)/(1+[\![e]\!]^((x-x0)/dx))$$

where A1 is initial value, A2 is final value, x0 is the inflection point and dx is lead concentration constant. The inflection point is useful for the evaluation of the affinity which quantifies how strong is the biomolecular interaction between PC6-AuNr and lead (II) ions in aqueous solutions: in our case, the x0 value is 73.6±0.9 $cm^{-1}ppb^{-1}$ corresponding to 1.8 x 10^{-10}±2 x 10^{-12} $cm^{-1}mol\ l^{-1}$.

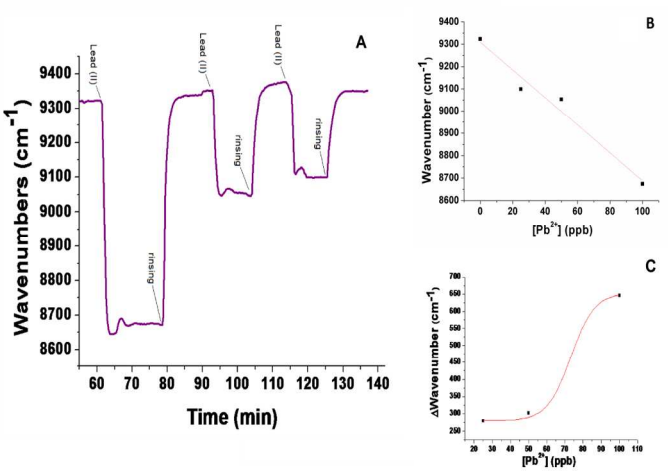

Figure 5. A) FT-SPR response as function of Lead (II) solutions concentration (respectively 100, 50 and 25ppb) during 3 cycles of binding followed by rinsing; B) SPR transmittance peak position by increasing concentration of lead solutions; C) SPR transmittance peak shift as function of Lead (II) solutions concentration.

CONCLUSIONS

In this work, we have characterized by optical, label free techniques the interaction between small peptides, namely PC6, and Pb (II) in aqueous solutions based on peptides adsorbed gold nanorods. These hybrids nanocomplexes are stable and biologically active: even if linked by adsorbed-gold interaction on the nanorods surface, the peptides are able to strongly bind the heavy metal ions with an affinity constant in the range of picomolar. The signal changes, i.e. variation of FT-SPR peak position, are important (more than 200 cm^{-1}) even at very low concentration (25 ppb) of metal ions: this result is very promising for development of sensitive and effective nanoparticle-based biosensor for quantifying Pb (II) ions concentration in water.

AUTHOR INFORMATION

Corresponding Author

* Jolanda Spadavecchia: jolanda.spadavecchia@upmc.fr

Author Contributions

The manuscript was written through contributions of all authors. / All authors have given approval to the final version of the manuscript. / ‡These authors contributed equally. (match statement to author names with a symbol)

Funding Sources

The present work is supported by Italian National Operative Program PON01_01525 "MONitoraggio Innovativo per le Coste e l'Ambiente marino".

REFERENCES

[1] Yavuz, M. S. ; Cheng, Y. ; Chen, J. ; Cobley, C. M.; Zhang, Q.; Rycenga, M. ; Xie, J. ; Kim, C.; Song, K. H;. Schwartz, A. G;. Wang, L. V; Xia, Y. Gold nanocages covered by smart polymers for controlled release with near-infrared light Nat. Mater. 2009, 8, 935–939.

[2] Giljohann, D. A. ; Seferos, D. S.; Daniel, W. L.; Massich, M. D.; Patel, P. C.; Mirkin, C. A. Gold nanopartikel in Biologie und Medizin Angew. Chem. 2010, 122, 3352–3366.

[3] Bedford, E. E.; Spadavecchia, J.; Pradier, C.-M.; Gu, F. X. Surface Plasmon Resonance Biosensors Incorporating Gold Nanoparticles Macromol. Biosci. 2012, 12, 724–739.

[4] Castellana , E.T.; Gamez , R. C.; Russell, D.H. J. Label-Free Biosensing with Lipid-Functionalized Gold Nanorods J. Am. Chem. Soc., 2011, 133 12, 4182–4185.

[5] Xia, N.; Shi, Y.; Zhang, R.; Zhao, F.; Liu F.; Liu L. Simple, rapid and label-free colorimetric assay for arsenic based on unmodified gold nanoparticles and a phytochelatin-like peptide Anal. Methods , 2012, 4, 3937–394.

[6] Rodríguez-Lorenzo, L.; De la Rica, R.; Álvarez-Puebla, R. A.; Liz-Marzán L.M. ;Stevens, M. M. Plasmonic nanosensors with inverse sensitivity by means of enzyme-guided crystal growth Nature Materials 2012,11, 604–607 .

[7] Zhenhai, G.; Jianhui, J.; Ting, Z.; Daocheng, W. J. Preparation of Rhodamine B Fluorescent Poly(methacrylic acid) Coated Gelatin Nanoparticles Nanomaterials, 2011, 1. 753705.

[8] Nikhil R. J.; Gearheart, L.;. Murphy C. J. Seed-Mediated Growth Approach for Shape-Controlled Synthesis of Spheroidal and Rod-like Gold Nanoparticles Using a Surfactant Template Advanced Materials, 2001, 13,18, 1389-1393.

[9] Harshala J Parab, J.-H. H; Lai, T.C.; Yi-Hua Jan, R.-S. L.;, Wang, J.L.; M. H., Y.-K. H. Chung-Hsuan Chen, Din Ping Tsai, S.-Y. C.;. Pang, J.-H. S. Biocompatible transferrin-conjugated sodium hexametaphosphate-stabilized gold nanoparticles: synthesis, characterization, cytotoxicity and cellular uptake Nanotechnology 2011, 22, 395706.

[10] Biver, T.; Eltugral, N.; Pucci, A.; Ruggeri, G.; Schena, A.; Secco, F.; Venturini, M. Synthesis, characterization, DNA interaction and potential applications of gold nanoparticles functionalized with Acridine Orange fluorophores Dalton Transactions, 40, 4190.

[11] Manson, J.; Kumar, D.; Meenan, B.; Dixon, D. Polyethylene glycol functionalized gold nanoparticles: the influence of capping density on stability in various media Gold Bulletin, 2011 44, 99.

[12] Zhao, H. ;Wu, S. Q.; Yao, Q.-H.; Xu, G.; Xu, Q. Nanocomposites containing gold nanorods and porphyrin-doped mesoporous silica with dual capability of two-photon imaging and photosensitization Langmuir, 2010 26, 14937.

[13] C.-J. L. Chang-HaiWang, Cheng-Liang Wang, Tzu-En Hua,, K. H. L. Judy M Obliosca, Y Hwu, Chung-Shi Yang,, H.-M. L. Ru-Shi Liu, Jung-Ho Je and G Margaritondo, J. Phys. D: Appl. Phys. 2008, 41, 195301.

[14] Shen, Q.; Nie, Z.; Guo, M.; Zhong, C.; Lin, B.; Li W.; Yao, S. Simple and rapid colorimetric sensing of enzymatic cleavage and oxidative damage of single-stranded DNA with unmodified gold nanoparticles as indicator Chem. Commun.,2009, 929-931.

[15] Tang, Y. L.; Feng, F. D.; He, S. F.; Wang, Li, Y. L.; Zhu, D. B. Direct Visualization of Enzymatic Cleavage and Oxidative Damage by Hydroxyl Radicals of Single-Stranded DNA with a Cationic Polythiophene Derivative J. Am. Chem. Soc., 2006, 128, 14972–14976.

[16] Li, W.; Nie, Z.; He, K.; Xu, X.; Li, Y.; Huang Y.; Yao, S. Simple, rapid and label-free colorimetric assay for Zn2+ based on unmodified gold nanoparticles and specific Zn2+ binding peptide Chem. Commun., 2011, 47, 4412–4414.

[17] Guo, Y.; Wang, Z.; Qu, W. ; Shao H.; Jiang, X. Colorimetric detection of mercury, lead and copper ions simultaneously using protein-functionalized gold nanoparticles Biosens. Bio-electron., 2011, 26, 4064–4069.

[18] Zhang, M.; Liu Y.-Q.; Ye, B.-C. Attomolar ultrasensitive microRNA detection by DNA-scaffolded silver-nanocluster probe based on isothermal amplification Analyst, 2012, 137, 601–607.

[19] Tong, S. Lead exposure and cognitive development: Persistence and a dynamic pattern J. Pediatr. Child Health 1998, 34, 114–118.

[20] Lilienthal, H.; Winneke, G.; Ewert, T. Effects of lead on neurophysiological and performance measures: animal and human data Environ Health Pers-pect. 1990, 89, 21–25.

[21] CDC, Surveillance for elevated blood lead levels among children-United States, 1997-2001. Centers for Disease Control and Prevention MMWR Morb Mortal Wkly Rep. 2003, 53, 1–21.

[22] Rothenberg, S.J.; Poblano, A.; Schnaas, L. Neurodegenerative Diseases and Metal Ions: Metal Ions in Life Sciences Neurotoxicol Tera-tol. 2000, 22, 503–510.

[23] Orita, M.; Iwahana, H.; Kanazawa, H.; Hayashi, K.; Sekiya, T. Detection of polymorphisms of human DNA by gel electrophoresis as single-strand conformation polymorphisms. Proc. Natl. Acad. Sci. USA, 86 (1989), 2766–2770.

[24] Cobbett , C.S.; Phytochelatin biosynthesis and function in heavy-metal detoxification. Current opinion in plant biology, 2000 , 3, 211–216.

[25] Manson, J. ; Kumar, D.; Meenan B. J.; Dixon, D. Polyethylene glycol functionalized gold nanoparticles: the influence of capping density on stability in various media, Gold Bull., 2011, 44, 99–105.

[26] Jana, N.R.; Gearheart, L.; Murphy, C.J. Seed-Mediated Growth Approach for Shape-Controlled Synthesis of Spheroidal and Rod-like Gold Nanoparticles Using a Surfactant Template Advanced Materials 2001, 13, 1389.

[27] Parab, H. J.; Huang, J.-H.; Lai, T.-C.; Jan, Y.-H.;. Liu, R.-S; Wang, J.-L.; Hsiao, M.; Chen, C.-H.;. Hwu, Y.-K.; Tsai, D. P.;

Chuang S.-Y.; S. Pang, J.-H. Biocompatible transferrin-conjugated sodium hexametaphosphate-stabilized gold nanoparticles: synthesis, characterization, cytotoxicity and cellular uptake. Nanotechnology, 2011, 22, 395706.

[28] Li, C.; Li, D.; Wan, G.; Xu J.; Hou, W. Facile synthesis of concentrated gold nanoparticles with low size-distribution in water: temperature and pH controls Nanoscale Res. Lett., 2011, 6, 440.

[29] Spadavecchia, J.; Moreau, J.; Hottin, J.; Canva, M. New cysteamine based functionalization for biochip applications Sens.Actuators, B 2009, 143, 139.

[30] Neoh K. G.; Kang, E. T. Functionalization of inorganic nanoparticles with polymers for stealth biomedical applications Polym. Chem., 2011, 2, 747.

[31] Gole, A.; Murphy, C.J. Seed-Mediated Synthesis of Gold Nanorods: Role of the Size and Nature of the Seed Chem. Materials 2004,16 , 3633.

[32] Busbee, B.D.; Obare, S.O.; Murphy, C.J. An Improved Synthesis of High-Aspect-Ratio Gold Nanorods Advanced Materials 2003,15, 414.

[33] Pérez-Juste, J.; Pastoriza-Santos, I.; Liz-Marzan, L.M.; Mulvaney, P. Gold nanorods: synthesis, characterization and applications Coord. Chem. Rev. 2005,249, 1870.

[34] Li, C.; Fan, F.; Yin, B.; Chen, L.; Ganguly, T.; Tian, Z. Au^{+}-cetyltrimethylammonium bromide solution: A novel precursor for seed-mediated growth of gold nanoparticles in aqueous solution Nano Research 2013, *6*, 29-37.

[35] Mattay, J. Photochemistry in Microheterogeneous Systems. Von K. Kalyanasundaram. Angewandte Chemie 1988,100,744.

[a]*Institute for Microelectronics and Microsystems, Unit of Naples-National Research Council Via P. Castellino 111, 80127 Italy*

[b]*Sorbonne Universités, UPMC Univ Paris 06, Laboratoire de Réactivité de Surface, 4 place Jussieu, F-75005 Paris, France.*

[c]*CNRS, UMR 7197, Laboratoire de Réactivité de Surface, F-75005, Paris, France*